Glycobiology vol. 17 no. 3 pp. 334–344, 2007
doi:10.1093/glycob/cwl078
Advance Access publication on December 19, 2006

Efficient introduction of a bisecting GlcNAc residue in tobacco *N*-glycans by expression of the gene encoding human *N*-acetylglucosaminyltransferase III

Gerard J.A. Rouwendal[1,3], Manfred Wuhrer[4], Dion E.A. Florack[3], Carolien A.M. Koeleman[4], André M. Deelder[4], Hans Bakker[2,3], Geert M. Stoopen[3], Irma van Die[5], Johannes P.F.G. Helsper[3], Cornelis H. Hokke[4], and Dirk Bosch[3,6]

[3]Business Unit Bioscience, Plant Research International B.V., Wageningen University and Research Centre, Droevendaalsesteeg 1 6708 PB Wageningen, The Netherlands; [4]Biomolecular Mass Spectrometry Unit, Department of Parasitology, Leiden University Medical Center, Albinusdreef 2, 2333 ZA Leiden, The Netherlands; [5]Glycoimmunology Group, Department of Molecular Cell Biology and Immunology, VU Medical Center, van der Boechorststraat 7, 1081 BT, Amsterdam, The Netherlands; and [6]Membrane Enzymology, Department of Chemistry, Utrecht University, Padualaan 8, 3584 CH, Utrecht, The Netherlands

Received on October 20, 2006; revised on December 1, 2006; accepted on December 5, 2006

In this study, we show that introduction of human *N*-acetylglucosaminyltransferase (GnT)-III gene into tobacco plants leads to highly efficient synthesis of bisected *N*-glycans. Enzymatically released *N*-glycans from leaf glycoproteins of wild-type and transgenic GnT-III plants were profiled by matrix-assisted laser desorption/ionization time-of-flight mass spectrometry (MALDI-TOF-MS) in native form. After labeling with 2-aminobenzamide, profiling was performed using normal-phase high-performance liquid chromatography with fluorescence detection, and glycans were structurally characterized by MALDI-TOF/TOF-MS and reverse-phase nano-liquid chromatography-MS/MS. These analyses revealed that most of the complex-type *N*-glycans in the plants expressing GnT-III were bisected and carried at least two terminal *N*-acetylglucosamine (GlcNAc) residues in contrast to wild-type plants, where a considerable proportion of *N*-glycans did not contain GlcNAc residues at the nonreducing end. Moreover, we have shown that the majority of *N*-glycans of an antibody produced in a plant expressing GnT-III is also bisected. This might improve the efficacy of therapeutic antibodies produced in this type of transgenic plant.

Key words: monoclonal antibody/electrospray ionization mass spectrometry/MALDI/*N*-glycosylation

Introduction

The initial steps of *N*-glycosylation of proteins in plants and animals, which take place in the endoplasmic reticulum, are very similar. However, on reaching the Golgi complex, this process starts to differ between and within both types of organisms, depending on tissue type and developmental stage. This variability is mainly the result of differences in the repertoire of Golgi-localized glycosyltransferases encoded by these organisms (Wilson 2002; Gomord and Faye 2004). A whole range of typical mammalian glycosyltransferases including, for example, β1,4-galactosyltransferase 1 (GalT) does not occur in plants, although human GalT can be expressed ectopically in tobacco plants using genetic modification as shown previously (Bakker, Bardor, et al. 2001; Bakker et al. 2006). Conversely, core β1,2-xylosyltransferase (XylT), for example, appears to be ubiquitous in plants, but seems to absent in most animals except snails and helminths (van Kuik et al. 1985; Khoo et al. 1997).

N-acetylglucosaminyltransferase III (GnT-III; EC 2.4.1.144) is one such animal enzyme that is lacking in plants. It is responsible for attaching a β1,4-linked *N*-acetylglucosamine (GlcNAc) residue to the β-linked mannose (Man) of the trimannosyl core; a structure that was first designated a bisecting GlcNAc in 1981 (Carver et al. 1981). A year before that, it was shown that the last two α1,2-linked Man residues from the hybrid $GlcNAc_2Man_5GlcNAc_2$, comprising a GlcNAc-linked β1,4 and a β-linked Man of the core, could not be removed by mannosidase II (Man-II), which would explain the existence of hybrid structures in ovalbumin (Harpaz and Schachter 1980b). In the *N*-glycosylation pathway, the action of GnT-III is preceded by GnT-I with $GlcNAcMan_5GlcNAc_2$ and $GlcNAc_2Man_3GlcNAc_2$ constituting the primary acceptors, whereas $GlcNAcMan_3GlcNAc_2$ is a relatively poor acceptor (Harpaz and Schachter 1980a; Narasimhan 1982; Schachter et al. 1983; Allen et al. 1984). The presence of a bisecting GlcNAc residue not only prevents the action of Man-II, but also the action of GnT II (Harpaz and Schachter 1980a), core α1,6-fucosyltransferase (FucT) (Longmore and Schachter 1982), and GnT-IV (Gleeson and Schachter 1983). In addition, it appears that steric hindrance due to the bisecting GlcNAc may cause reduced galactosylation of the α1,3 arm, although GalT is not completely prevented from functioning unlike the above-mentioned enzymes (Narasimhan et al. 1985). On the other hand, GnT-III activity is completely inhibited by the presence of a β1,4-linked galactose (Gal) attached to the GlcNAc residue of the α1,3-arm of $GlcNAc_2Man_3GlcNAc_2$ (Schachter et al. 1983).

The gene encoding the rat GnT-III was the first one of its kind to be cloned and was later found to be 91% identical to its human homolog at the amino acid level (Nishikawa et al.

[1]To whom correspondence should be addressed; e-mail: gerard.rouwendal@wur.nl
[2]Present address: Abteilung Zelluläre Chemie, Medizinische Hochschule Hannover, Carl-Neuberg-Strasse 1, Hannover, Germany.

1992; Ihara et al. 1993). Overexpression of GnT-III in Chinese hamster ovary (CHO) cells used for the production of a monoclonal antibody (mAb) caused high levels of bisected *N*-glycans, which improved the therapeutic value of the product by increasing its antibody-dependent cellular cytotoxicity (ADCC) activity (Umana et al. 1999). The goal of this study was to explore the possibility of introducing bisecting GlcNAc residues on plant N-linked glycans through the ectopic expression of a GnT-III gene. In addition, we wanted to examine whether this would lead to reductions in core-bound xylose (Xyl) and fucose (Fuc) on *N*-glycans of endogenous proteins and an antibody produced in the transgenic plants.

Using matrix-assisted laser desorption/ionization time-of-flight mass spectrometry (MALDI-TOF-MS), we provide evidence that almost all *N*-glycans in tobacco plants expressing the human GnT-III gene are bisected and contain core-bound Xyl. The most remarkable observation, however, was the virtual lack of paucimannosidic structures that are commonly found in wild-type plants. In addition, through reverse-phase nano-liquid chromatography (LC)-MS/MS of glycopeptides of a recombinant antibody produced in a plant expressing GnT-III, we showed that the majority of its *N*-glycans were also bisected and devoid of paucimannosidic structures.

Results

Selection of transgenic tobacco plants expressing the human GnT-III *gene*

The gene encoding the human GnT-III was introduced in tobacco plants by *Agrobacterium*-mediated transformation of the binary vector pBINPLUSGnT-III, containing a copy DNA (cDNA) harboring the complete coding sequence fused to a C-terminal cellular homolog of myelocytomatosis viral oncogene (c-myc) tag under control of the constitutive cauliflower mosaic virus 35S (CaMV35S) promoter. Sixty independent kanamycin-resistant transgenic shoots were obtained; of which, 16 were rooted and transferred to the greenhouse. An immunoblot assay with anti-c-myc antibodies revealed that all transformants displayed similar levels of GnT-III (data not shown). However, it proved to be very difficult to obtain stable progeny with the transgenic trait and only line GnT-III-20-2 has been retained.

Western blot analysis of GnT-III-20-2

Rabbit anti-HRP antibodies bind very strongly and specifically to typical plant *N*-glycans, and this antibody and its affinity-purified fractions with anti-Xyl and anti-Fuc specificity were used to analyze line GnT-III-20-2 (Kurosaka et al. 1991). Leaf proteins from line GnT-III-20-2 were compared with leaf proteins from wild-type plants by western blot analysis (Figure 1). A steep decline in antibody binding to protein from GnT-III-20-2 leaves was observed in the second lanes of each of the three panels in Figure 1, as compared with the signal from wild-type plants in the first lanes. This suggests that GnT-III expression caused a considerable decrease in the levels of core-bound Xyl and Fuc.

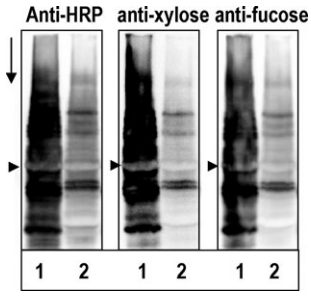

Fig. 1. Western blot of total protein from wild-type (lanes 1) and transgenic tobacco lines GnT-III-20-2 (lanes 2). The blots were probed with rabbit anti-HRP antibodies and purified fractions thereof containing anti-Xyl and anti-Fuc antibodies. The position of the small subunit of ribulose-1,5-biphosphate carboxylase/oxygenase is indicated with an arrowhead and the arrow points in the direction of electrophoresis.

Activity of Arabidopsis thaliana *XylT and FucT with bisected acceptor*

As several mammalian enzymes are inhibited by the presence of a bisecting GlcNAc residue, the plant core β1,2-XylT and core α1,3-FucT (FucT-C3-1) were also tested for their ability to employ an acceptor with bisecting GlcNAc. To this end, the cloned cDNAs corresponding to the *Arabidopsis* FucT-C3-1 and β1,2-XylT were expressed in CHO cells and homogenates of these cells were tested for activity with a number of acceptors (Table I). Core α1,3-FucT displayed full activity with the biantennary acceptor, but almost no activity with its bisected version. Core β1,2-XylT was incapable of using this bisected acceptor and had optimal activity with $GlcNAcMan_3GlcNAc_2$. Hence, both enzyme preparations were active with their preferred substrates, but displayed hardly, if any, activity with a bisected substrate.

N-glycan profile of GnT-III expressing plant

Proteins were isolated from tobacco wild-type and GnT-III-20-2 plants, cleaved with pepsin, and the *N*-glycans were released using peptide *N*-glycosidase A. Released glycans were labeled with 2-aminobenzamide (2-AB), and glycan profiles of wild-type and GnT-III-20-2 plants were compared by normal phase high-performance liquid chromatography (HPLC) with fluorescence detection and this revealed marked differences (Figure 2). Eluting species were analyzed by MALDI-TOF-MS after peak fractionation. Oligosaccharide compositions were deduced from the observed masses. Based on the plant origin of the glycans and the specificity of the glycosyltransferases involved in *N*-glycosylation, hexoses, *N*-acetylhexosamines, deoxyhexoses, and pentoses were interpreted as Man, GlcNAc, Fuc, and Xyl, respectively.

The HPLC profile for line GnT-III-20-2 showed three major peaks (Figure 2B). A comparison of the HPLC profile with the MALDI-TOF MS indicated that the latter also provided an adequate reflection of the actual *N*-glycan make-up (Figure 3; Harvey 2003). For two of the peaks (at 92.0 and 100.3 min), no corresponding peak was detected in the wild-type run (Figure 2A). On the basis of their composition, the species $GlcNAc_3(Xyl)Man_3GlcNAc_2$ (at 92.0 min) and $GlcNAc_3(Xyl)(Fuc)Man_3GlcNAc_2$ (at 100.3 min) were assumed to be bisecting. For the species $GlcNAc_2(Xyl)Man_3GlcNAc_2$ (87.8 min), a MALDI-TOF/TOF-MS analysis

Table I. Acceptor specificity of *Arabidopsis thaliana* recombinant glycosyltransferases α1,3-FucT-C3-1 and β1,2-XylT

Acceptor	Diagram	Enzyme activity (pmol/min per mg protein)	
		FucT	XylT
GlcNAcβ1-2Manα1-3(Manα1-6)Manß-OR	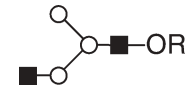	ND	48 (100%)
GlcNAcβ1-2Manα1-3(GlcNAcβ1-2Manα1-6)Manβ1-4GlcNAcβ1-4(Fucα1-6)GlcNAc–GP	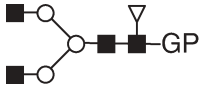	168 (100%)	40 (82%)
GlcNAcβ1-2Manα1-3(GlcNAcβ1-2Manα1-6) (GlcNAcβ1-4)Manβ1-4GlcNAcβ1-4(Fucα1-6)GlcNAc–GP	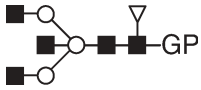	3 (2%)	—

R, O-$(CH_2)_8$-$COOCH_3$; GP, IgG glycopeptide; ND, not determined.

[precursor of mass to charge ratio (m/z) 1569.9] produced diagnostic ions at m/z 1407.8, 1042.2, 910.3, and 701.2 that are in accordance with a bisected *N*-glycan structure, but cannot be explained based on a biantennary *N*-glycan (Figure 4).

Reverse phase nano-LC-MS of the 2-AB labeled $GlcNAc_2(Xyl)(Fuc)Man_3GlcNAc_2$ fraction from GnT-III-20-2 revealed the presence of two isobaric species, with one being approximately 50 times more abundant than the other (data not shown). The retention times of both species differed from that of $GlcNAc_2(Xyl)(Fuc)Man_3GlcNAc_2$ from the wild-type plant. Differences in fragmentation patterns between wild-type derived $GlcNAc_2(Xyl)(Fuc)Man_3GlcNAc_2$ and the isobaric species from the GnT-III plant are shown in Figure 5. The doubly-protonated species at m/z 858 was fragmented in the ion-trap (IT) MS and the singly-charged fragment resulting from loss of a GlcNAc was fragmented further. The spectra differed considerably and, in Figure 5B, a range of ions at m/z 569.1, 910.3, and 1072.3 can be observed that are typical of a bisected precursor fragment. The high intensity of the ion at m/z 1309.5 in Figure 5A compared with that in Figure 5B and the relatively low intensity of the ion at m/z 1025.3 in Figure 5A compared with that in Figure 5B demonstrate the high stability of the bisecting GlcNAc. The signal at m/z 1171.3 seems to arise from Fuc rearrangements, which are known to occur on

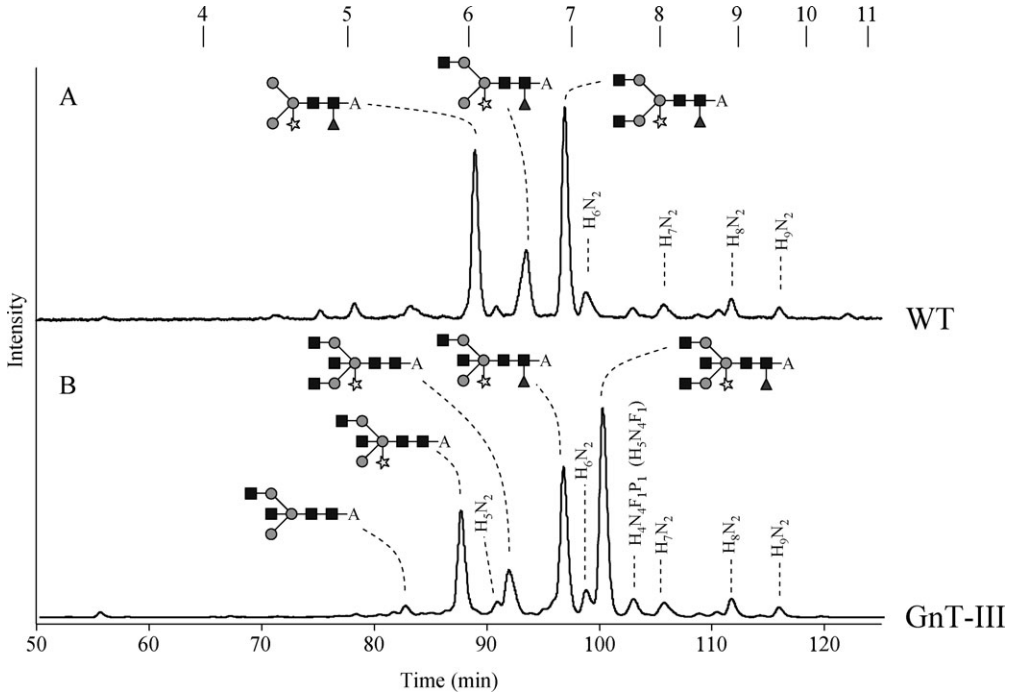

Fig. 2. Normal phase HPLC analysis of 2-AB-labeled N-linked glycans isolated (**A**) from leaves of wild-type tobacco plant (WT) and (**B**) from leaves of transgenic plant GnT-III-20-2 (GnT-III). Compositions and structural schemes of the *N*-glycan peaks as identified by MALDI-TOF (see Figure 3) are given in terms of hexose (circle), *N*-acetylhexoxamine (square), Fuc (triangle), and Xyl (star). Elution positions of 2-AB-labeled dextran oligomers are indicated at the top by vertical lines together with the degree of polymerization. A, 2-AB label.

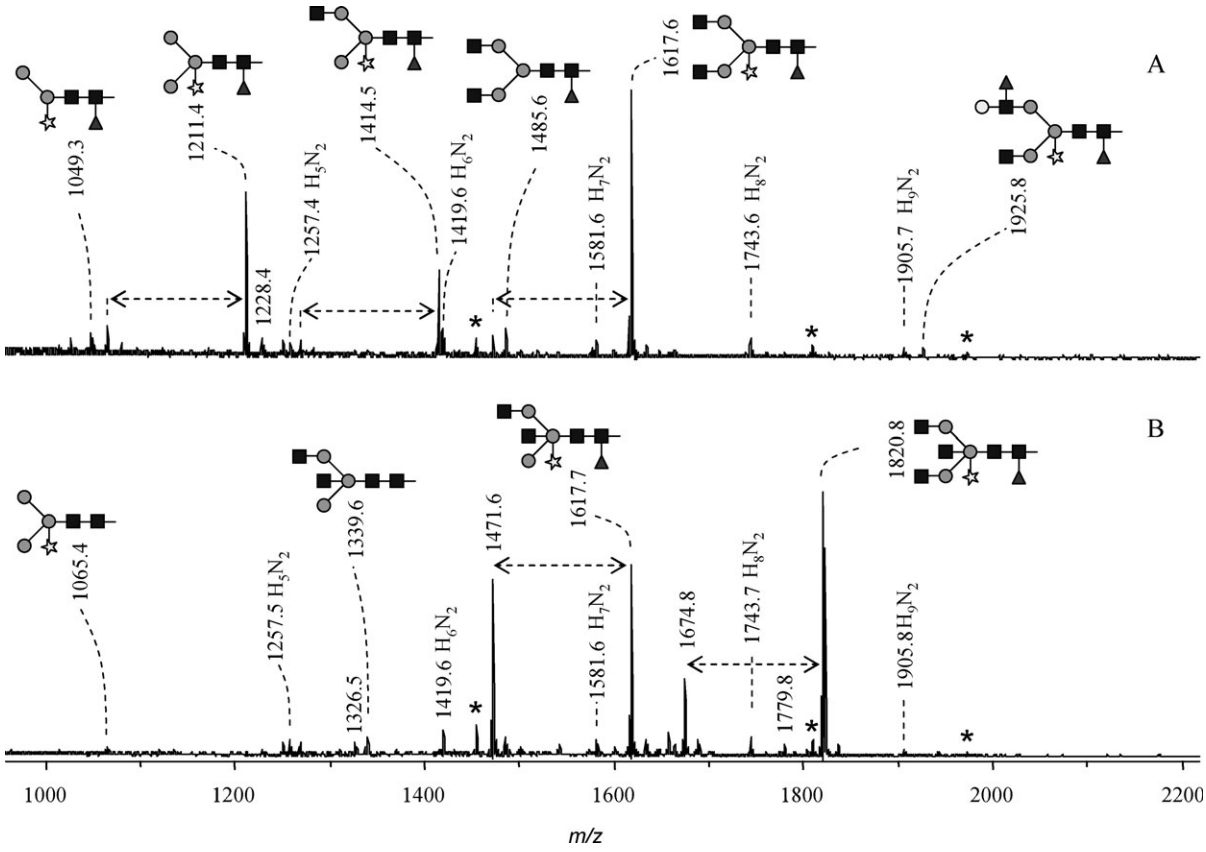

Fig. 3. MALDI-TOF MS analysis of N-linked glycans isolated (**A**) from leaves of wild-type tobacco plant (WT) and (**B**) from leaves of transgenic plant GnT-III-20-2 (GnT-III). Compositions and structural schemes are given in terms of hexose (circle), *N*-acetylhexoxamine (square), Fuc (triangle), Xyl (star). Glycans were registered in unlabeled, native form as sodium adducts. Masses are given rounded to 1 decimal place. *, contaminant.

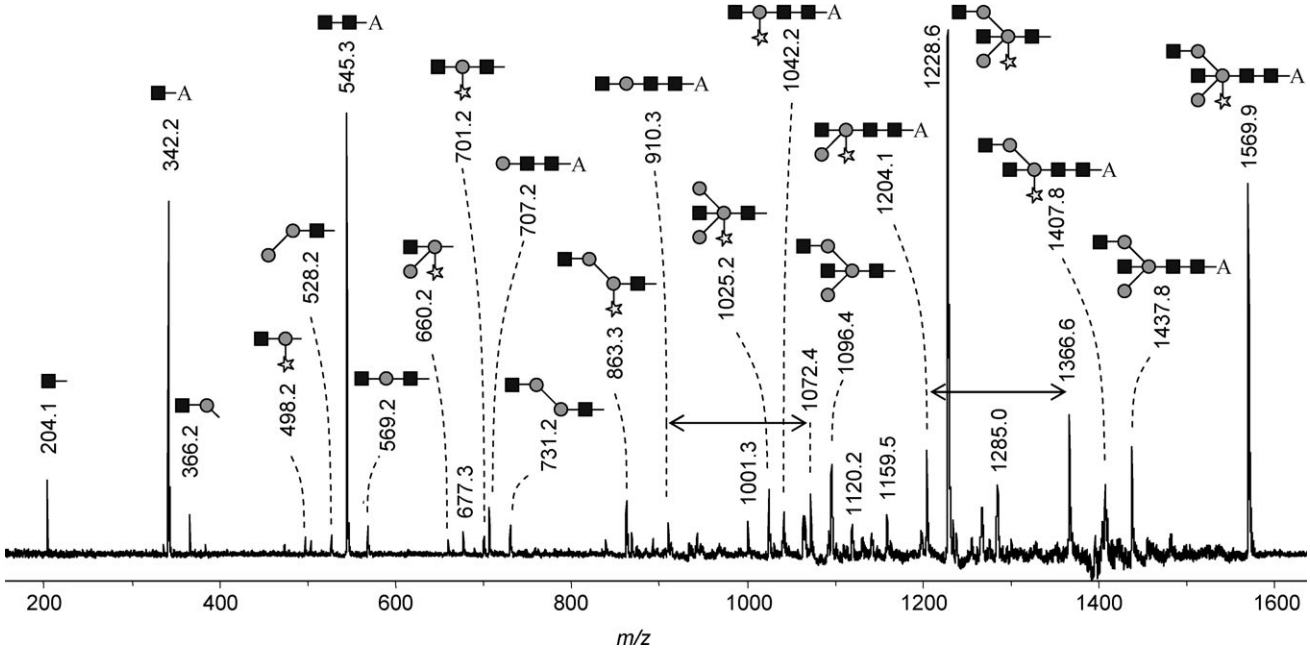

Fig. 4. MALDI-TOF/TOF-MS of the 2-AB-labeled glycan species $H_3N_4P_1$ derived from transgenic line GnT-III-20-2. The chromatographic peak at 87.8 min (Figure 2B) was collected and analyzed by MALDI-TOF-MS (not shown). The registered proton adduct at m/z 1569 was analyzed for fragment ions by MALDI-TOF/TOF-MS. Masses are given rounded to 1 decimal place. Double-headed arrows indicate differences in hexose content. For key, see Figure 3.

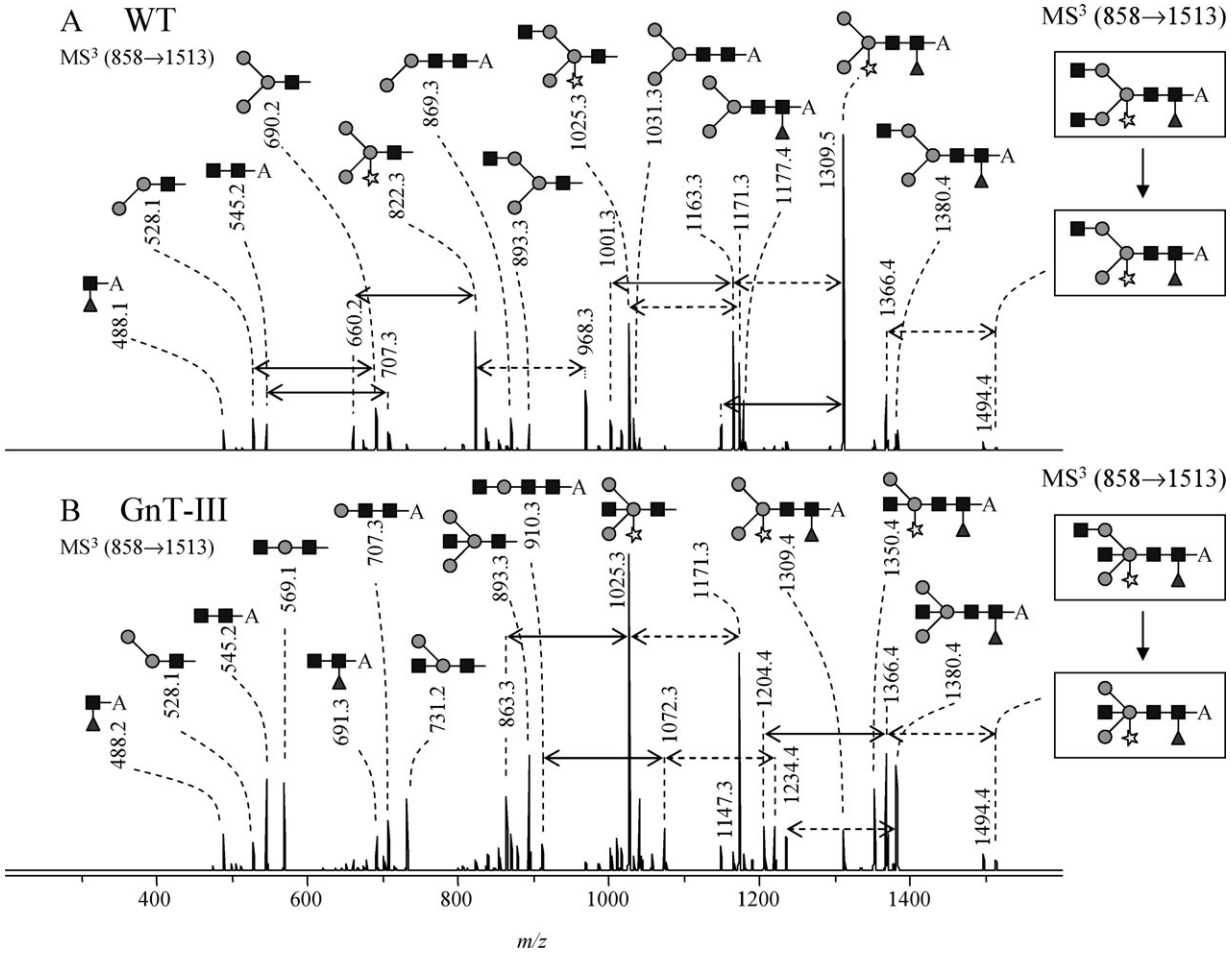

Fig. 5. Fragment ion analysis of 2-AB-labeled $H_3N_4F_1P_1$. 2-AB-labeled $H_3N_4F_1P_1$ species of wild-type (**A**) and transgenic (**B**) tobacco GnT-III-20-2 plants were analyzed by nano-LC-MS/MS/MS. Doubly-protonated species (m/z 858) were isolated and fragmented in the ion-trap MS. The singly-charged fragment at 1513 m/z arising from loss of an *N*-acetylhexosamine was isolated and fragmented, resulting in the given fragment ion spectra. Masses are given rounded to 1 decimal place. Double-headed arrows with continuous and dashed lines indicate differences in *N*-acetylhexosamine and Fuc content, respectively. For key, see Figure 3.

collision-induced dissociated proton adducts (Wuhrer, Koeleman, Hokke, et al. 2006 and references therein).

N-glycan composition of antibody from GnT-III expressing plant

In order to study the *N*-glycan profile of an antibody produced in a transgenic line expressing GnT-III, we created a series of new transgenics using the original gene cassette built into a plant transformation vector with a hygromycin resistance marker to allow re-transformation of an existing kanamycin-resistant tobacco plant producing antibody MGR48 (Smant et al. 1997). A typical line expressing both GnT-III and the antibody was selected from a small group of six transgenics using western blot analysis with anti-HRP and anti-immunoglobulin G (IgG) probes, respectively (data not shown). A MALDI-TOF MS analysis of unlabeled *N*-glycans from these six lines showed that in all of them between 65% and 75% of *N*-glycans were in the form of $GlcNAc_3Man_3(Xyl)(Fuc)GlcNAc_2$ (data not shown). Antibody MGR48 was purified from the selected line GIIIMGR5 using protein G and it was shown by sodium dodecyl sulfate–polyacrylamide gel electrophoresis (SDS–PAGE) analysis to be slightly degraded as was found previously for the same antibody from wild-type tobacco plants (data not shown; Stevens et al. 2000).

Glycosylation of the antibody MGR48 purified from GnT-III-expressing tobacco plants was analyzed at the level of tryptic glycopeptides by nano-LC-electrospray ionization (ESI)-IT-MS. The obtained glycopeptide profile for the single *N*-glycosylation site of the antibody is shown in Figure 6. In order to be able to register a representative glycopeptide profile, the voltages of the ion transfer region of the mass spectrometer were optimized to avoid in-source decay of the protonated glycoconjugates. Loss of terminal monosaccharides in the ion transfer region can be excluded, as no oxonium ions arising, for example, from chitobiose cleavage were observed in the low mass region. Likewise, no loss of Fuc was observed for the major glycan species (m/z 1469 in Figure 6; loss of Fuc would result in a signal at m/z 1396.0, which is not observed), though Fuc is known to be easily lost under harsh ion transfer conditions. On the basis of these considerations, it may be concluded that the observed glycopeptide profile (Figure 6) represents native glycan species. MS/MS experiments (Figure 7 and data not shown) showed that the

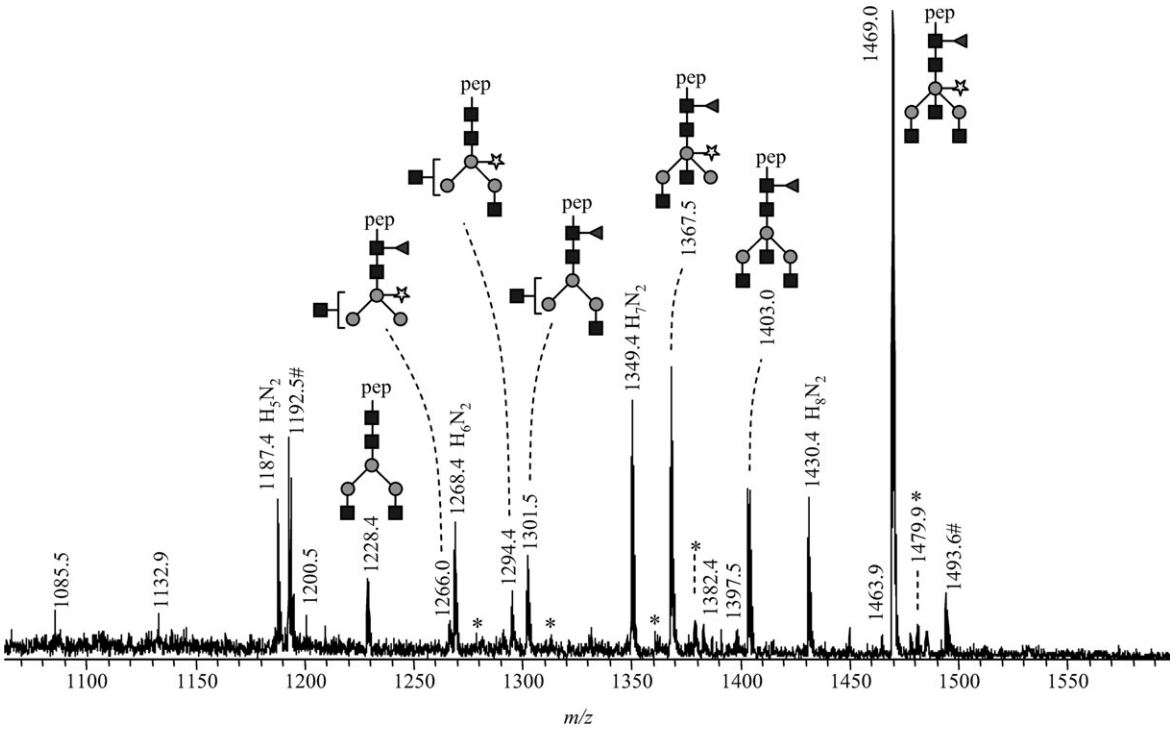

Fig. 6. Nano-LC-ESI-IT-MS of the tryptic glycopeptides from MGR48 expressed in tobacco line GnT-III-20-2. Structures were assigned based on the combination of obtained glycopeptide MS/MS data (see Figure 7) and of deduced structures of released glycans from total tobacco leaf glycoproteins. Glycopeptides were observed as doubly-protonated species. Monoisotopic masses are given rounded to 1 decimal place. For key see Figure 3; #, singly-charged species (not glycopeptide related).

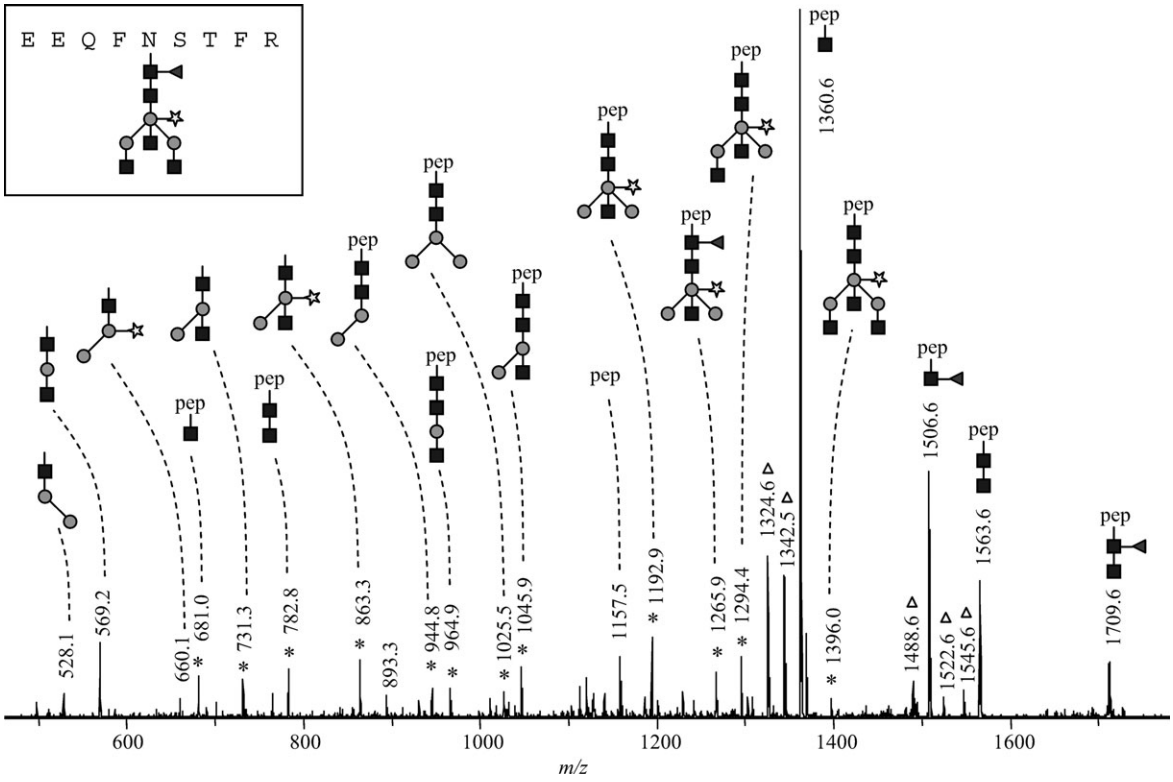

Fig. 7. Nano-LC-ESI-IT-MS/MS of the most abundant tryptic glycopeptide of MGR48 expressed in tobacco line GnT-III-20-2.The tryptic glycopeptide registered at m/z 1469 (Figure 6) was subjected to automatic fragment ion analysis using collision-induced dissociation in the IT MS. Singly- and doubly-protonated fragment ions were observed, and monoisotopic masses are given rounded to 1 decimal place. For key, see Figure 3; Δ, elimination of water and/or ammonia. *, double-charged ion.

majority of *N*-glycans linked to the constant region of antibody molecule (Fc) of the heavy chain were bisected. For example, fragment ion analysis of the most abundant tryptic glycopeptide at m/z 1469.0 revealed the presence of two ions at m/z 569.2 and 964.9, both of which are typical of bisected structures (Figure 7). However, in contrast to the complex-type *N*-glycans from endogenous proteins in line GnT-II-20-2, which were all bisected, at least one of the antibody *N*-glycans from line GIIIMGR5 at m/z 1228.4 was not bisected as determined by fragment ion analysis (data not shown). Moreover, in contrast to *N*-glycans from total protein from line GnT-III-20-2, the oligosaccharides from the antibody contained clearly detectable amounts of bisected species in which the only core-bound substitution consisted of Fuc. In addition, high-Man-type *N*-glycans appeared to be more prevalent in the antibody than in the glycoprotein content as a whole.

Discussion

To our knowledge, the synthesis of bisected *N*-glycans in transgenic tobacco plants expressing the human GnT-III gene reported here is only the second example of typical animal *N*-glycans being synthesized in transgenic plants (Palacpac et al. 1999; Bakker, Bardor, et al. 2001). The *N*-glycan profile of the GnT-III-20-2 line is made up of four major complex-type *N*-glycans, two of which are definitely biantennary with a bisecting GlcNAc, as judged by their m/z value. The other two also contained a bisecting GlcNAc, as was shown by detailed MALDI-TOF/TOF MS and nano-LC-MS/MS analyses. Hence, we conclude that most complex-type *N*-glycans in this line are bisected. The extraordinarily high level of this type of oligosaccharide in this line, as well as in the other randomly selected transgenics expressing the mAb, suggests that the enzyme acts very efficiently in a plant cell environment.

The absence of hybrid *N*-glycans could mean either that GnT-III does not act at early stages of Golgi-localized *N*-glycosylation or that plant Man-II and GnT-II are able to cope with the bisected acceptors $GlcNAc_2Man_5GlcNAc_2$ and $GlcNAc_2Man_3GlcNAc_2$, respectively. This is in contrast to their animal counterparts (Harpaz and Schachter 1980b; Allen et al. 1984; Bendiak and Schachter 1987). Support for the hypthesis of a late-acting GnT-III came from the observations that both the core β1,2-XylT and FucT-C3-1 could not function with a bisected, biantennary acceptor, while all complex *N*-glycans contained core-bound Xyl and frequently Fuc as well. Consequently, addition of Xyl and Fuc probably preceded that of a bisecting GlcNAc. Further support for a late-acting GnT-III can be deduced from the observation that efficient xylosylation requires core β1,2-XylT to act before core α1,3-FucT, and since core β1,2-XylT is concentrated mainly in the medial-Golgi compartment, core α1,3-FucT is then likely to be localized beyond this compartment and possibly in the vicinity of GnT-III (Pagny et al. 2003; Bencúr et al. 2005). The colocalization of FucT and GnT-III is also corroborated by the presence of a substantial fraction of *N*-glycans lacking core-bound Fuc in GnT-III plants relative to wild-type plants. This suggests that GnT-III regularly prevails over core α1,3-FucT and that the distribution of GnT-III and core α1,3-FucT in transgenic plants is overlapping. In mammalian cells, GnT-III activity must be restricted to the later stages of *N*-glycosylation in the trans-Golgi compartment, as it would otherwise interfere with proper processing of *N*-glycans to biantennary molecules. Interference with normal processing can be inferred, for example, from experiments in which a chimeric GnT-III, comprising the N-terminal cytoplasmic transmembrane stem (CTS)-region from a medial-Golgi enzyme expressed in mammalian cells and purportedly shifting localization to earlier stages of *N*-glycosylation, caused the formation of hybrid *N*-glycans (Ferrara, Brünker, et al. 2006). All in all, it is likely that human GnT-III produced in plant cells is also localized in the trans-Golgi compartment similar to core FucT (Fitchette-Lainé et al. 1994).

High levels of bisected $GlcNAc_2$ $(Xyl)Man_3GlcNAc_2$ and $GlcNAc_2(Xyl)(Fuc)Man3GlcNAc2$ peaks are due to either removal of a GlcNAc residue from one of the arms or incomplete processing. Unfortunately, we do not know the identity of the two isobaric 2-AB-labeled $GlcNAc_2(Xyl)Man_3$ $GlcNAc_2$ species found in GnT-III-20-2, one of which being present in trace amounts compared with the other. In one species, the GlcNAc of the α1,3-arm seems to be missing, whereas in the other, the GlcNAc of the α1,6 arm is absent. As addition of Xyl, Fuc, and bisecting GlcNAc depend on the presence of the GlcNAc on the α1,3-arm, lack of GlcNAc linked to the α1,3-arm in any $GlcNAc_2(Xyl)Man_3GlcNAc_2$ species must be due to the action of an hexosaminidase (Tezuka et al. 1992; Leiter et al. 1999). Two insect hexosaminidases have been discovered that preferentially, or even exclusively, remove the β1,2-linked GlcNAc from the Man(α1,3)-arm and homologous *Arabidopsis* hexosaminidase genes have been identified (Léonard et al. 2006; Tomiya et al. 2006). The isobaric species without the GlcNAc on the α1,6-arm could be due to degradation of $GlcNAc_3(Xyl)$ $Man_3GlcNAc_2$ by hexosaminidase activity as well, but we could not rule out a defect in biosynthesis whereby addition of a bisecting GlcNAc immediately following the actions of Man-II, core β1,2-XylT, and core α1,3-FucT might create an acceptor that would be as unsuitable for the plant GnT-II as it would be for its animal counterpart (Bendiak and Schachter 1987). Irrespective of the exact configuration of the bisected *N*-glycans in which one of the antennae is missing a GlcNAc residue, it is clear that the typical wild-type paucimannosidic *N*-glycans $(Xyl)(Fuc)Man_3GlcNAc_2$ and $GlcNAc(Xyl)(Fuc)Man_3GlcNAc_2$) are completely lacking in the GnT-III plants. Apparently, the bisecting residue provides considerable protection to the hexosaminidase-mediated cleavage of GlcNAc on one of the antennae.

Previously, we have shown that expression of a hybrid GalT (β1,4-GalT) in tobacco caused a sharp reduction in the binding of anti-HRP to proteins of those transgenic plants concomitant with a strong reduction in the levels of core-bound Xyl and Fuc residues in their *N*-glycans (Bakker et al. 2006). Although the lack of anti-HRP binding to proteins from line GnT-III-20-2 also suggested a strong reduction in core-bound Xyl and Fuc residues, the MALDI-TOF MS data demonstrated unequivocally that reduced binding was very likely due to shielding of the core-bound epitopes by both terminal GlcNAc residues and not to a decline of the levels of core-bound Xyl and Fuc. Indeed, even wild-type biantennary *N*-glycans with terminal GlcNAc on both antennae already lead to severe steric hindrance of antibody binding (Bencúrová et al. 2004).

Coexpression of genes encoding GnT-III and a therapeutic antibody in mammalian human embryonic kidney 293-Epstein–Barr virus nuclear antigen cells yields antibodies with hybrid and complex glycans, most of which are bisected and fucosylated. In this expression system, the use of a chimeric GnT-III with the CTS region of Man-II yields antibodies with bisected, hybrid glycans that are almost completely devoid of core-bound Fuc and achieve a highly increased ADCC compared with the unmodified antibody (Shields et al. 2002; Shinkawa et al. 2003; Ferrara, Brünker, et al. 2006). High-affinity binding of glyco-engineered nonfucosylated antibodies to FcγRIIIA may be due to the fact that the receptor is able to approach the Fc more closely in the absence of the α1,6-Fuc. It is unknown how the interaction between plant-made antibodies with *N*-glycans substituted with α1,3-Fuc or β1,2-Xyl and the FcγRIIIA receptor is affected, let alone in the presence of a bisecting GlcNAc.

Earlier analyses of MGR48 produced in wild-type tobacco have already shown that the *N*-glycans of this antibody contained much less core-bound substitutions than the endogenous glycoproteins (Elbers et al. 2001). In fact, production of MGR48 in a glyco-engineered tobacco expressing a hybrid GalT gene yielded antibodies with little, if any, *N*-glycans containing core-bound Xyl and Fuc (Bakker et al. 2006). The nano-LC-ESI-IT-MS analysis of tryptic EEQFNSTFR-glycopeptides from MGR48 prepared from a GnT-III expressing line showed that a major fraction contained one or both core modifications in addition to a significant fraction carrying high-Man-type *N*-glycans. The occurrence of slightly higher levels of high-Man-type *N*-glycans linked to MGR48 antibodies has been observed before and appeared to be highest in antibody preparations from relatively young upper leaves (Elbers et al. 2001). The fact that MGR48 antibody from the GnT-III expressing plant did comprise an *N*-glycan species with Fuc as the only core substitution is somewhat remarkable, because this structure did not occur to a significant extent on total protein. Hence, as far as *N*-glycan synthesis on MGR48 antibody in a GnT-III plant is concerned, and especially with respect to the role of core β1,2-XylT, core α1,3-FucT, and GnT-III, compartmentalization of these glycosyltransferases appears to be much less distinct than in *N*-glycan synthesis on the whole. For example, in order to arrive at the glycopeptides at m/z 1301.5 and 1403.0 (Figure 6), the supposedly late-acting GnT-III must have acted earlier than XylT, which has been shown to accumulate in the medial-Golgi compartment. Nevertheless, the most abundant glycopeptide carried a bisected *N*-glycan with both core modifications indicating that in this case, XylT and FucT acted before GnT-III. It remains to be seen whether the core α1,3-Fuc, characteristic of the majority of plant *N*-glycans on antibody molecules from GnT-III expressing plants, interferes with high-affinity binding of such an antibody to FcγRIIIa in the same way as the core α1,6-Fuc found in mammalian IgG antibodies (Ferrara, Stuart, et al. 2006).

Materials and methods

Plasmids and plant transformation

The human gene for GnT-III was cloned from P1-derived artificial chromosome (PAC) clone RPI5-1104-E15 by polymerase chain reaction using AccuTaq LA DNA polymerase (Sigma-Aldrich, Zwijadrecht, The Netherlands) and primers GNT3F (5′-TACTCGAGTTAACAATGAAGATG-AGACGCT-3′) and GNT3Rmyc (5′-TATGGATCCTAA TTCAGAT CCTCTTCTGAGATGAG-3′). The resulting fragment was cloned in *Eco*RV site of pBluescribe SK+ (Stratagene, La Jolla, CA) and the sequence was verified. A 1.6 kb *Hpa*I/*Bam*HI fragment containing the GnT-III gene with C-terminal c-myc tag was subsequently cloned into the *Sma*I/*Bgl*II site of pUCAP35S (van Engelen et al. 1995). The CaMV35S promoter expression cassette with modified GnT-III gene was subsequently cloned as a *Asc*I/*Pac*I fragment either in the binary vector pBINPLUS or in the pMOG22, which had been modified to contain a multiple cloning site flanked by *Asc*I/*Pac*I sites (van Engelen et al. 1995; Goddijn et al. 1993). The vectors were introduced in *Agrobacterium tumefaciens* strains Agl0 or LBA4404, respectively, by electroporation. Transformation of *Nicotiana tabacum* variety Samsun NN wild-type or homozygous transgenic plants MGR48-31-4 producing the mAb MGR48 was carried out as described before (Bakker, Bardor, et al. 2001; Bakker et al. 2006). Transgenic plants were selected and grown to maturity in the greenhouse at 21°C.

Western blot analysis

Protein extracts were prepared by grinding two leaf discs per plant to fine powder in a 1.5 mL Eppendorf tube under liquid nitrogen. For lectin blotting, 250 μL of SDS–PAGE loading buffer [20 mM Tris–HCl, pH 6.8, 6% (v/v) glycerol, 0.4% (w/v) SDS, 2.5 μg/mL bromophenol blue] containing 5% (v/v) β-mercaptoethanol was mixed with the frozen powder, and the contents were boiled immediately for 5 min. The samples were centrifuged for 2 min at 20 800*g* and 17.5 μL of supernatant was loaded onto a 10% SDS–PAGE gel. Protein was transferred onto nitrocellulose as described previously (Faye et al. 1993; Bakker, Bardor, et al. 2001; Bakker, Schijlen, et al. 2001). Equal loading was verified using Ponceau S staining of the blot. Immunological detection of plant glycoproteins was performed with rabbit anti-HRP-IgG (Rockland, Gilbertsville, PA) and Xyl- and Fuc-specific fractions thereof followed by HRP-conjugated goat anti-rabbit-IgG (Bakker, Bardor, et al. 2001). Signals were visualized using chemiluminescent substrate Lumi-Light (Roche Diagnostics, Almere, The Netherlands) and a Roche Diagnostics Lumi-Imager.

Enzyme assays

Nonsialylated core α1,6-fucosylated glycopeptides from human IgG (ag-GP-IgGF_6) were prepared essentially as described in Narasimhan et al. (1979). The glycopeptides were degalactosylated by treatment with jack bean β-galactosidase (1 unit/10 μmol glycopeptide). Glycopeptides containing a bisecting GlcNAc were separated from glycopeptides without a bisecting GlcNAc as described in Narasimhan et al. (1986). CHO cells were transiently transfected with pABE-At-FucT-C3-1 and pABE-At-XylT cDNA using the calcium phosphate precipitation method (Bakker, Schijlen, et al. 2001). FucT and XylT assays were performed in a 25 μL reaction mixture containing 2.5 μmol sodium cacodylate (pH 7.0), 0.25 μmol $MnCl_2$, 0.1 μmol ATP, 2.5 nmol GDP-[^{14}C]Fuc (2 Ci/mol) or UDP-[^{14}C]Xyl (4 Ci/mol), 0.1% (v/v) Triton

X-100, 1 mM acceptor substrate, and 5–10 μL of CHO cell homogenate, as described previously (van Tetering et al. 1999). Control assays lacking the acceptor substrate were carried out to correct incorporation into endogenous acceptors. After incubation for 60–120 min at 37 °C, the reaction was stopped and the product was separated from unincorporated label by chromatography on a 1 mL column of Dowex-1-X8 according to Nemansky and Van den Eijnden (1993).

MALDI-TOF(/TOF)-MS

MALDI-TOF(/TOF)-MS data were obtained using an Ultraflex I TOF-MS (Bruker, Daltonics, Bremen, Germany) equipped with a LIFT-MS/MS facility. 6-Aza-2-thiothymine (5 mg/mL; Sigma-Aldrich) was used as a matrix. Spectra were acquired in the positive ion reflectron mode. For fragment ion analysis in the tandem (TOF/TOF) mode, precursors were accelerated to 8 kV and selected in a timed ion gate. Fragment ions arising from metastable decomposition of the precursor were further accelerated by 19 kV in the LIFT cell, and their masses analyzed after the ion reflector passage. External calibration of MALDI-TOF mass spectra was carried out using singly-charged monoisotopic peaks of a mixture of human angiotensin I, bombesin, adrenocorticotropic hormone (ACTH 18-39), and somatostatin-28 (Bruker, Daltonics). For MALDI-TOF/TOF-MS, calibrations were performed using fragment ion spectra obtained for the proton adducts of these peptides.

Normal phase HPLC and reverse phase-nano-LC-MS/MS of 2-AB-labeled glycans

N-glycans were purified as described previously (Bakker et al. 2006). Labeling of glycans with 2-AB and normal phase-HPLC analysis with fluorescence detection was performed as described before (Wuhrer et al. 2004). Peak-fractions were collected and analyzed by MALDI-TOF (/TOF)-MS [see *MALDI-TOF(/TOF)-MS* section] and reverse phase nano-LC-MS/MS as described previously (Wuhrer, Koeleman, Deelder, et al. 2006).

Glycopeptide analysis

MGR48 antibody purified from GnT-III-expressing plants was incubated with 1 μg trypsin (Promega, Leiden, The Netherlands) at 37 °C overnight (Bakker, Bardor, et al. 2001). The resulting (glyco-)peptide samples were applied to a reverse-phase column (C18 PepMap 100 Å, 3 μm, 75 μm × 150 mm; Dionex/LC Packings, Amsterdam, The Netherlands) using an Ultimate nano-LC system, a Famos autosampler, and a Switchos trap-column system (Dionex/LC Packings). The column was equilibrated at room temperature with eluent A (0.1% formic acid in water) at a flow rate of 150 nL/min. After injection of the sample, a gradient was applied to 50% eluent B (95% acetonitrile and 0.1% formic acid) in 30 min followed by an isocratic elution with 50% eluent B for 15 min. The eluate was monitored by absorption at 215 nm.

The LC column was coupled to an Esquire HCT ultra ESI-IT-MS (Bruker, Daltonics) equipped with an online nanospray source operating in the positive ion mode. For electrospray (1100–1250 V), capillaries (360 μm outer diameter, 20 μm inner diameter with 10 μm opening) from New Objective (Cambridge, MA) were used. The solvent was evaporated at 175 °C employing a nitrogen stream of 7 L/min. Ions from m/z 200 to 2500 were registered. When operated in the auto-MS/MS mode, each MS scan was followed by the acquisition of MS/MS spectra of up to three of the most abundant ions in the MS spectrum.

Acknowledgments

The authors wish to thank Dr Pieter de Jong (Children's Hospital Oakland Research Institute) for the kind gift of PAC clone RPI5-1104-E15, Dr Kerr Anderson (The Dow Chemical Company) for helpful discussions, and Dr Robert Hall (Plant Research International) for reading the manuscript. UDP-[^{14}C]Xylose was a kind gift from Prof. Dr H. Kamerling (University of Utrecht). This work was financially supported by Wageningen University and Research Center and The Dow Chemical Company. All experiments involving genetically modified organisms were performed according to licenses GGO97-230 and 00-138 from the Ministry of Housing, Spatial Planning and the Environment.

Conflict of interest statement

None declared.

Abbreviations

2-AB, 2-Aminobenzamide; ADCC, antibody-dependent cellular cytotoxicity; CaMV35S, cauliflower mosaic virus 35S; cDNA, copy DNA; CHO, Chinese hamster ovary; c-myc, cellular homolog of myelocytomatosis viral oncogene; CTS, cytoplasmic transmembrane stem; ESI, electrospray ionization; Fc, constant region of antibody molecule; Fuc, fucose; FucT, fucosyltransferase; Gal, galactose; GalT, β1,4-galactosyltransferase 1; GlcNAc, *N*-acetylglucosamine; GnT, *N*-acetylglucosaminyltransferase; HPLC, high-performance liquid chromatography; HOD, horseradisch peroxidase; IgG, immunoglobulin G; IT, ion trap; LC, liquid chromatography; mAb, monoclonal antibody; MALDI, matrix-assisted laser desorption/ionization; Man, mannose; Man-II, mannosidase II; MS, mass spectrometry; m/z, mass to charge ratio; PAC, P1-derived artificial chromosome; SDS–PAGE, sodium dodecyl sulfate–polyacrylamide gel electrophoresis; TOF, time-of-flight; UDP, uridine diphosphate; Xyl, xylose; XylT, xylosyltransferase

References

Allen SD, Tsai D, Schachter H. 1984. Control of glycoprotein synthesis. The in vitro synthesis by hen oviduct membrane preparations of hybrid asparagines-linked oligosaccharides containing 5 mannose residues. J Biol Chem. 259:6984–6990.

Bakker H, Bardor M, Molthoff JW, Gomord V, Elbers I, Stevens LH, Jordi W, Lommen A, Faye L, Lerouge P, et al. 2001. Galactose-extended glycans of antibodies produced by transgenic plants. Proc Natl Acad Sci USA. 98:2899–2904.

Bakker H, Schijlen E, de Vries T, Schiphorst WE, Jordi W, Lommen A, Bosch D, van Die I. 2001. Plant members of the alpha1 → 3/4-fucosyltransferase gene family encode an alpha1 → 4-fucosyltransferase, potentially involved in Lewis(a) biosynthesis, and two core alpha1 → 3-fucosyltransferases. FEBS Lett. 507:307–312.

Bakker H, Rouwendal GJA, Karnoup AS, Florack DEA, Stoopen GM, Helsper JPFG, van Ree R, van Die I, Bosch D. 2006. An antibody produced in tobacco expressing a hybrid β-1,4-galactosyltransferase is essentially devoid of plant carbohydrate epitopes. Proc Natl Acad Sci USA. 103:7577–7582.

Bendiak B, Schachter H. 1987. Control of glycoprotein synthesis. Kinetic mechanism, substrate specificity, and inhibition characteristics of UDP-*N*-acetylglucosamine:α-D-mannoside β1-2 *N*-acetylglucosaminyltransferase II from rat liver. J Biol Chem. 262:5784–5790.

Bencúr P, Steinkellner H, Svoboda B, Mucha J, Strasser R, Kolarich D, Hann S, Köllensperger G, Glössl J, Altmann F, et al. 2005. *Arabidopsis thaliana* ß1,2-xylosyltransferase: an unusual glycosyltransferase with the potential to act at multiple stages of the plant *N*-glycosylation pathway. Biochem J. 388:515–525.

Bencúrová M, Hemmer W, Focke-Tejkl M, Wilson IBH, Altmann F. 2004. Specificity of IgG and IgE antibodies against plant and insect glycoprotein glycans determined with artificial glycoforms of human transferring. Glycobiology. 14:457–466.

Carver JP, Grey AA, Winnik FM, Hakimi J, Ceccarini C, Atkinson PH. 1981. Determination of the structure of four glycopeptides from hen ovalbumin using 360-MHz magnetic resonance spectroscopy. Biochemistry. 20:6600–6606.

Elbers IJW, Stoopen GM, Bakker H, Stevens LH, Bardor M, Molthoff JW, Jordi WJRM, Bosch D, Lommen A. 2001. Influence of growth conditions and developmental stage on N-glycan heterogeneity of transgenic immunoglobulin G and endogenous proteins in tobacco leaves. Plant Physiol. 126:1314–1322.

Faye L, Gomord V, Fitchette-Lainé A-C, Chrispeels MJ. 1993. Affinity purification of antibodies specific for Asn-linked glycans containing α1 → 3 fucose or ß1 → 2 xylose. Anal Biochem. 209:104–108.

Ferrara C, Brünker P, Suter T, Moser S, Püntener U, Umaña P. 2006. Modulation of therapeutic functions by glycosylation engineering: influence of Golgi enzyme localization domain and co-expression of heterologous ß1,4-N-acetylglucosaminyltransferase III and Golgi α-mannosidase II. Biotechnol Bioeng. 93:851–861.

Ferrara C, Stuart F, Sondermann P, Brünker P, Umaña P. 2006. The carbohydrate at FcγRIIIa Asn-162. An element required for high affinity binding to non-fucosylated IgG glycoforms. J Biol Chem. 281: 5032–5036.

Fitchette-Lainé A-C, Gomord V, Chekkafi A, Faye L. 1994. Distribution of xylosylation and fucosylation in the plant Golgi apparatus. Plant J. 5: 673–682.

Florack DEA, Dirkse WG, Visser B, Heidekamp F, Stiekema WJ. 1994. Expression of biologically active hordothionins in tobacco. Effects of pre- and pro-sequences at the amino and carboxyl termini of the hordothionin precursor on mature protein expression and sorting. Plant Mol Biol. 24: 83–96

Gleeson PA, Schachter H. 1983. Control of glycoprotein synthesis. J Biol Chem. 258:6162–6173.

Goddijn OJM, Lindsey K, van der Lee FM, Klap JC, Sijmons PC. 1993. Differential gene expression in nematode-induced feeding structures of transgenic plants harbouring promoter—*gus*A fusion constructs. Plant J. 4:863–873.

Gomord V, Faye L. 2004. Posttranslational modification of therapeutic proteins in plants. Curr Opin Plant Biol 7:171–181.

Harpaz N, Schachter H. 1980a. Control of glycoprotein synthesis. Bovine colostrum UDP-*N*-acetylglucosamine:alpha-D-mannoside β2-*N*-acetylglucosaminyltransferase I. Separation from UDP-*N*-acetylglucosamine:α-D-mannoside β2-*N*-acetylglucosaminyltransferase II, partial purification, and substrate specificity. J Biol Chem. 255:4885–4893.

Harpaz N, Schachter H. 1980b. Control of glycoprotein synthesis. Processing of asparagine-linked oligosaccharides by one or more rat liver Golgi alpha-D-mannosidases dependent on the prior action of UDP-N-acetylglucosamine: α-D-mannoside β2-*N*-acetylglucosaminyltransferase I. J Biol Chem. 255:4894–4900.

Harvey DJ. 2003. Matrix-assisted laser desorption/ionization mass spectrometry of carbohydrates and glycoconjugates. Int J Mass Spectrom. 226:1–35.

Ihara Y, Nishikawa A, Tohma T, Soejima H, Niikawa N, Taniguchi N. 1993. cDNA cloning, expression, and chromosomal localization of human *N*-acetylglucosaminyltransferase III (GnT-III). J Biochem (Tokyo) 113: 692–698.

Khoo K-H, Chatterjee D, Caulfield JP, Morris HR, Dell A. 1997. Structural mapping of the glycans from the egg glycoproteins of *Schistosoma mansoni* and *Schistosoma japonicum*: identification of novel core structures and terminal sequences. Glycobiology. 7:663–677.

Kurosaka A, Yano A, Itoh N, Kuroda Y, Nakagawa T, Kawasaki T. 1991. The structure of a neural specific carbohydrate epitope of horseradisch peroxidase recognized by anti-horseradish peroxidase antiserum. J Biol Chem. 266:4168–4172.

Leiter H, Mucha J, Staudacher E, Grimm R, Glössl J, Altmann F. 1999. Purification, cDNA cloning, and expression of GDP-L-Fuc:Asn-linked GlcNAc α1,3-fucosyltransferase from mung beans. J Biol Chem. 274: 21830–21839.

Léonard R, Rendic D, Rabouille D, Wilson IBH, Préat T, Altmann F. 2006. The *Drosophila* fused lobes gene encodes an *N*-acetylglucosaminidase involved in *N*-glycan processing. J Biol Chem. 281:4867–4875.

Longmore GD, Schachter H. 1982. Product-identification and substrate-specificity studies of the GDP-L-fucose:2-acetamido-2-deoxy-β-D-glucoside(Fuc → Asn-linked GlcNAc) 6-α-L-fucosyltransferase in a Golgi-rich fraction from porcine liver. Carbohydr Res. 100:365–392.

Narasimhan S. 1982. Control of glycoprotein synthesis. J Biol Chem. 257: 10235–10242.

Narasimhan S, Freed JC, Schachter H. 1985. Control of glycoprotein synthesis. Biochemistry. 24:1694–1700.

Narasimhan S, Freed J, Schachter H. 1986. The effect of a "bisecting" *N*-acetylglucosaminyl group on the binding of biantennary, complex oligosaccharides to concanavalin A, *Phaseolus vulgaris* erythroagglutinin (E-PHA), and *Ricinus communis* agglutinin (RCA-120) immobilized on agarose. Carbohydr Res. 149:65–83.

Narasimhan S, Wilson JR, Martin E, Schachter H. 1979. A structural basis for four distinct elution profiles on concanavalin A–Sepharose affinity chromatography of glycopeptides. Can J Biochem. 57:83–96.

Nemansky M, Van den Eijnden DH. 1993. Enzymatic characterization of CMP-NeuAc:Gal beta 1-4GlcNAc-R alpha(2–3)-sialyltransferase from human placenta. Glycoconj J. 10:99–108.

Nishikawa A, Ihara Y, Hatakeyama M, Kangawa K, Taniguchi N. 1992. Purification, cDNA cloning, and expression of UDP-*N*-acetylglucosamine:β-D-mannoside β-1,4*N*-acetylglucosaminyltransferase III from rat kidney. J Biol Chem. 267:18199–18204.

Pagny S, Bouissonnie F, Sarkar M, Follet-Gueye ML, Driouich A, Schachter H, Faye L, Gomord V. 2003. Structural requirements for *Arabidopsis* beta1,2-xylosyltransferase activity and targeting to the Golgi. Plant J. 33:189–203.

Palacpac NQ, Yoshida S, Sakai H, Kimura Y, Fujiyama K, Yoshida T, Seki T. 1999. Stable expression of human β1,4-galactosyltransferase in plant cells modifies N-linked glycosylation patterns. Proc Natl Acad Sci USA. 96: 4692–4697.

Schachter H, Narasimhan S, Gleeson P, Vello G. 1983. Control of branching during the biosynthesis of asparagines linked oligosaccharides. Can J Biochem Cell Biol. 61:1049–1066.

Shields RL, Lai J, Keck R, O'Connell LY, Hong K, Meng YG, Weikert SHA, Presta LG. 2002. Lack of fucose on human IgG1 N-linked oligosaccharide improves binding to human FcγRIII and antibody-dependent cellular toxicity. J Biol Chem. 30:26733–26740.

Shinkawa T, Nakamura K, Yamane N, Shoji-Hosaka E, Kanda Y, Sakurada M, Uchida K, Anazawa H, Satoh M, Yamasaki M, et al. 2003. The absence of fucose but not the presence of galactose of bisecting N-acetylglucosamine of human IgG1 complex-type oligosaccharides shows the critical role of enhancing antibody-dependent cellular cytotoxicity. Proc Natl Acad Sci USA. 278:3466–3473.

Smant G, Goverse A, Stokkermans JPWG, De Boer JM, Pomp H, Zilverentant JF, Overmars HA, Helder J, Schots A, Bakker J. 1997. Potato root diffusate-induced secretion of soluble basic proteins originating from the subventral esophageal glands of potato cyst nematodes. Phytopathology 87:839–845.

Stevens LH, Stoopen GM, Elbers IJW, Molthoff JW, Bakker HAC, Lommen A, Bosch D, Jordi W. 2000. Effect of climate conditions and plant developmental stage on the stability of antibodies expressed in transgenic tobacco. Plant Physiol. 124:173–182.

Tezuka K, Hayashi M, Ishihara H, Akazawa T, Takahashi N. 1992. Studies on synthetic pathway of xylose-containing N-linked oligosaccharides deduced from substrate specificities of the processing enzymes in sycamore cells (*Acer pseudoplatanus* L.). Eur J Biochem. 203: 401–413.

Tomiya N, Narang S, Park J, Abdul-Rahman B, Choi O, Singh S, Hiratake J, Sakata K, Betenbaugh MJ, Palter KB, et al. 2006. Purification, characterization, and cloning of a *Spodoptera frugiperda* Sf9 β-*N*-acetylhexosaminidase that hydrolyzes terminal *N*-acetylglucosamine on the *N*-glycan core. J Biol Chem. 281:19545–19560.

Umana P, Jean-Mairet J, Moudry R, Amstutz H, Bailey JE. 1999. Engineered glycoforms of an antineuroblastoma IgG1 with optimized antibody-dependent cellular cytotoxic activity. Nat Biotechnol. 17:176–180.

van Engelen FA, Molthoff JW, Conner AJ, Nap J-P, Pereira A, Stiekema WJ. 1995. pBINPLUS: An improved plant transformation vector based on pBIN19. Transgenic Res. 4:288–290.

van Kuik JA, van Halbeek H, Kamerling JP, Vliegenthart JFG. 1985. Primary structure of the low-molecular-weight carbohydrate chains of *Helix pomatia* α-hemocyanin. J Biol Chem. 260:13984–13988.

van Tetering A, Schiphorst WE, van den Eijnden DH, van Die I. 1999. Characterization of a core alpha1 → 3-fucosyltransferase from the snail *Lymnaea stagnalis* that is involved in the synthesis of complex-type N-glycans. FEBS Lett. 461:311–314.

Wilson IBH. 2002. Glycosylation of proteins in plants and invertebrates. Curr Opin Struct Biol. 12:569–577.

Wuhrer M, Koeleman CAM, Deelder AM, Hokke CH. 2006. Repeats of LacdiNAc and fucosylated LacdiNAc on N-glycans of the human parasite *Schistosoma mansoni*. FEBS J. 273:347–361.

Wuhrer M, Koeleman CAM, Hokke CH, Deelder AM. 2006b. Mass spectrometry of proton adducts of fucosylated N-glycans: fucose transfer between antennae gives rise to misleading fragments. Rapid Commun Mass Spectrom. 20:1747–1754.

Wuhrer M, Robijn MLM, Koeleman CAM, Balog CIA, Geyer R. Deelder AM, Hokke CH. 2004. A novel Gal(beta1-4)Gal(beta1-4)Fuc (alpha1-6)-core modification attached to the proximal N-acetylglucosamine of keyhole limpet haemocyanin (KLH) N-glycans. Biochem J. 378:625–632.